Paul J. Keller, PhD • William W. Hunter, Jr., MD • Petra Schmalbrock, PhD

Multisection Fat-Water Imaging with Chemical Shift Selective Presaturation[1]

Proton chemical shift imaging yielding separate water and lipid images was performed in a multisection mode on a clinical 1.5-T whole-body magnetic resonance imaging unit. Imaging was performed with a minor modification of the standard multisection spin-warp technique: that is, the addition of a sinc pulse or a soft square pulse and a homospoil gradient at the beginning of the pulse sequence. Phantom and human anatomic images are presented.

Index terms: Magnetic resonance (MR), chemical shift • Magnetic resonance (MR), technology

Radiology 1987; 164:539-541

PROTON chemical shift imaging leading to the production of separate water- and lipid-based images has been accomplished by several methods (1-12). T2 weighting alone yields a certain amount of fat-water discrimination. Specific techniques that have been described previously include those based on chemical shift selective pulses (1-5), on phase difference discrimination (6), on variation of frequency encoding gradients (7, 8), and on selection by multiple quantum coherence (9). The availability of these methods has led to their application in the diagnosis of clinical disease.

One of the chief hindrances to wider application of fat-water imaging is that most of the heretofore available pulse sequences suitable for large-bore clinical magnetic resonance (MR) imaging units yield only single-section chemical shift images or require computer postprocessing. A multisection technique using stimulated echoes has been elegantly demonstrated on a small-bore instrument (3). We describe a simple presaturation method for multisection fat-water imaging on a clinical MR imaging unit. Implementation of this technique requires only minor modification of the standard multisection spin-echo imaging pulse sequence.

MATERIALS AND METHODS

The basic technique involves appending a radio frequency (RF) pulse and a "homospoil" gradient immediately before the beginning of each excitation pulse sequence (Fig. 1). It is well known that the power spectrum of a time-domain square pulse is a (sine x)/x function (also known as a sinc function) centered at the RF carrier frequency (ω_0). With the RF carrier frequency set on either the water or the lipid resonance the width of the square pulse is adjusted such that PW = $n/\Delta\delta$, where PW is the pulse width of this square RF pulse, $n = 1, 2, 3, \ldots$, and $\Delta\delta$ is the chemical shift difference (in hertz) between the water and lipid signals. When these RF pulse characteristics are selected, a null in the power spectrum of the square pulse occurs at the frequency of the off-resonance signal. The chemical shift difference between water and lipid at 1.5 T is $\Delta\delta$ = 210 Hz, which corresponds to an RF pulse width PW = 4.8 msec for the first null (n = 1). The amplitude of the square pulse is selected to yield a $\pi/2$ pulse for the on-resonance peak. This simple calculation does not yield the exact position of the null as would a more rigorous rotating frame analysis (13), but the error introduced is small in comparison with the line-widths encountered.

The effect of the square pulse is the conversion of the bulk z-magnetization into xy-magnetization of the on-resonance signal, whereas for the off-resonance peak the bulk magnetization remains along the z-axis. A homospoil gradient is then applied, which dephases the xy-magnetization. Thus, no coherent magnetization as a result of the on-resonance signal remains. At this point, execution of the usual spin-warp excitation sequence gives only signals that originate from the off-resonance peak.

Interleaved multisection image acquisition is normally accomplished with exclusive use of section selective pulses. This permits nuclear relaxation to occur in sections recently excited while excitation/detection sequences are being performed in other sections. The addition of a spatially nonselective presaturation pulse to the sequence does not interfere with multisection acquisition because the signal forming the image is not excited by this pulse. The presaturation pulse and the homospoil are repeated before every section excitation in a given repetition time (TR), insuring that little or no longitudinal magnetization from the saturated component is present.

The procedure was performed with a Signa clinical MR imaging system (General Electric Medical Systems, Milwaukee) equipped with a 1-m bore superconducting magnet operating at 1.5 T. Interleaved multisection spin-warp images were obtained of a 150 ml Griffen beaker containing aqueous $CuSO_4$ and cooking oil with use of the head volume coil of the system. The sinc pulse presaturation

[1] From the Departments of Radiology and Chemistry (P.J.K.), the Ohio State University, Columbus. From the 1986 RSNA annual meeting. Received December 5, 1986; revision requested February 20, 1987; revision received March 10; accepted March 24. **Address reprint requests to** P.J.K., MRI Facility, Barrow Neurological Institute, 350 W. Thomas Rd., Phoenix, AZ 85013.

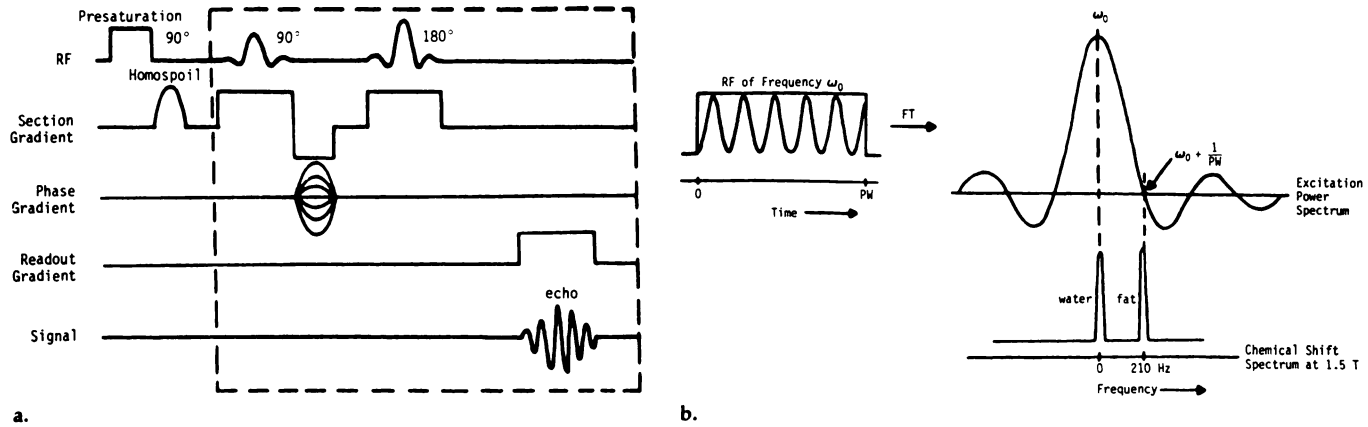

Figure 1. **(a)** Modification of multisection spin-warp imaging sequence for use in fat-water imaging. The relationship between time and frequency domains of a square pulse and the chemical shifts of fat and water resonances are shown. **(b)** The actual frequencies of the nulls are more rigorously calculated by a rotating frame analysis $\Delta f = \{[(2n\pi/PW)^2 - (\gamma H_1)^2]^{1/2}\}/2\pi$, where $n = 1, 2, 3, \ldots$, indicating which 0 crossing is being calculated, and $PW\gamma H_1$ is assumed to equal a 90° pulse on resonance (13). For the 4.8 msec pulse discussed in the text, this analysis yields the first null at ±202 Hz from ω_0 rather than ±208 Hz as predicted by $\omega_0 \pm 1/PW$, an error of approximately 3%. This error decreases by a factor of n as n increases. *FT* = Fourier transform.

sequence was used to image the right knee, spine, and head of a healthy human volunteer. The body volume coil was used for RF transmission and a rectangular (32 × 18-cm) surface coil was used for reception.

RESULTS

A critical analysis of the chemical shift images of the water- and oil-filled beaker (Fig. 2) reveals two types of imperfections: (*a*) decreased signal-to-noise ratios (S/N) compared with S/N of the normal nonselective image and (*b*) small image intensity variations across regions containing the selected substance as well as across regions containing the suppressed substance. These problems are largely attributable to B_0 inhomogeneity over the volume of the sample; for example, in the case of the water image, the center of the water resonance is positioned at the null in the power spectrum of the square pulse. However, since B_0 inhomogeneity results in spatial variation of the precise water resonance frequency, this yields a certain degree of excitation for water resonating at frequencies on either side of the center of the overall water signal. This phenomenon accounts for both aforementioned imperfections.

One obvious remedy is to double the length of the square pulse in order to place the water resonance (again, the case of water image production) on the second null from the middle of the power spectrum. The amplitude of the pulse would be decreased by a factor of two, retaining the $\pi/2$ flip angle on resonance. This approach takes advantage of the decreased slope on either side of the second versus the first null. In turn, variations in B_0 would have a smaller effect on the amount of water *z*-magnetization remaining after presaturation. However, the B_0 inhomogeneity problem for the signal to be suppressed (here lipid) is exacerbated by this approach because of the narrowing of the high amplitude region of the power spectrum, which leads to greater flip angle variations for the same degree of B_0 inhomogeneity.

A superior alternative solution replaces the square pulse with a sinc time domain pulse, which ideally yields a square power spectrum. This reduces flip angle variation across both of the signals. In practice, it was found that a sinc pulse played out over $\pm\pi$ in 8 msec gave satisfactory results. These values predict a bandwidth of approximately ±125 Hz; thus the power spectrum approaches 0 amplitude approximately halfway between the water and lipid signals. This is similar to the technique of Bottomley et al. (1), except that the homospoil and the section selective π pulse permit multisection operation.

Figures 3 and 4 display normal, fat, and water images of the right knee and spine, respectively, of a healthy human volunteer. Some signal from adipose tissue is still seen in the water image, but adipose tissue is not free of water. Moreover, olefinic lipid protons are not suppressed when this method is used. Figure 5 shows axial images obtained in the head of a volunteer. The signal in the center of the brain is indistinguishable from noise, which indicates good water suppression of the lipid images. An artifact resulting from susceptibility effects is observed near the ethmoid sinus.

DISCUSSION

The technique described in this report has several advantages over competing methods. The clinician may select TR and echo time values in the usual fashion and obtain images that,

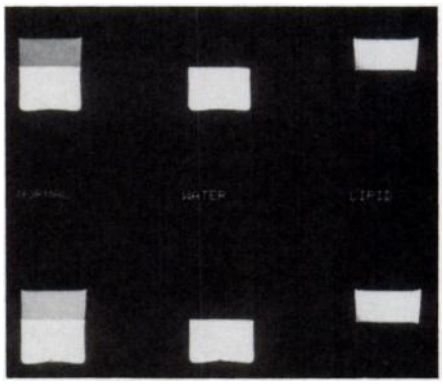

Figure 2. Normal (left), water (center), and fat (right) images of a beaker containing aqueous $CuSO_4$ and cooking oil; two of five simultaneously acquired sections are shown. Note the drop of oil at the bottom of the beaker in the image at bottom right.

except for the suppression of the fat or water component, closely resemble the standard spin-warp values. Our method does not rely on the ability to superimpose exactly two image matrices for subtraction. It is compatible with multisection, multiecho acquisitions that use arbitrary echo times. It is simple to implement and requires no unusual postprocessing of the image data.

The chief detracting feature of our method lies in its dependence on B_0 homogeneity for signal selection. The same is true of other published methods, except for double quantum filtration (9). The magnet homogeneity of our system is usually sufficient for fat-water imaging across a set of sections spanning up to about 4 cm (field of view = 24 cm) without active shimming. Obviously the greater the imaging volume is, the more severe the B_0 inhomogeneity is. Another potential problem is bulk susceptibility effects on B_0 in the region of air-tissue interfaces, like that observed for the lipid

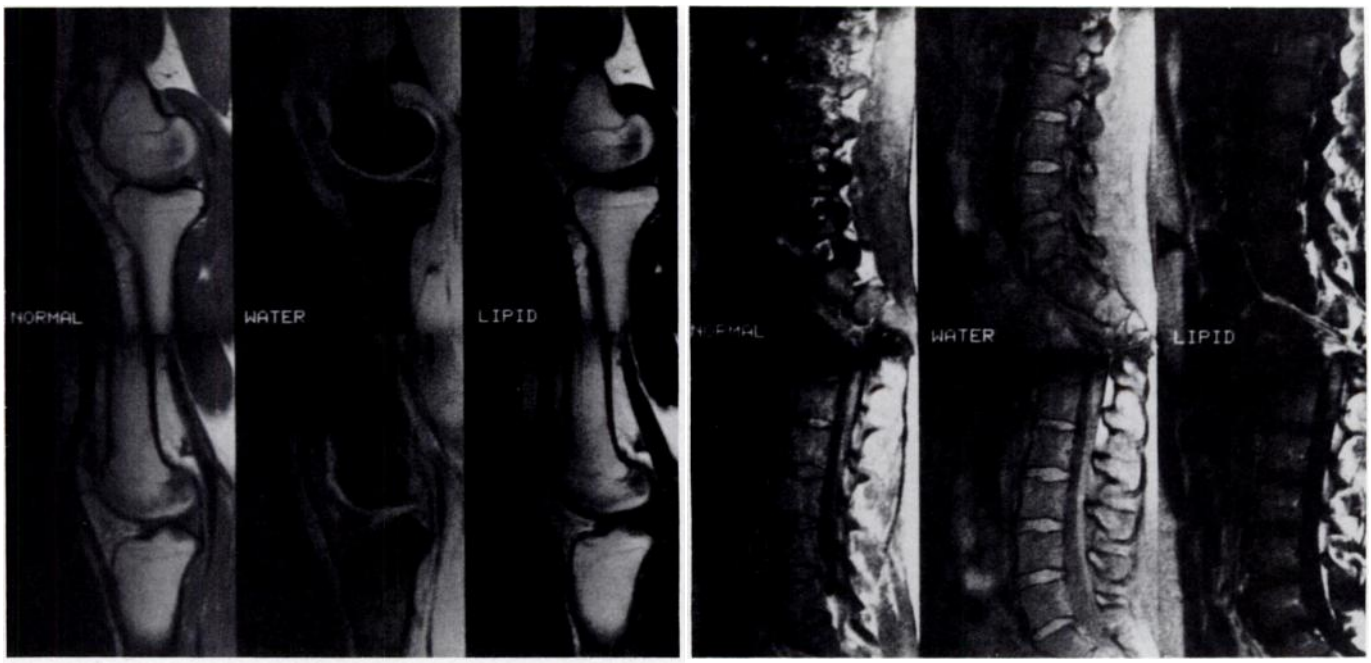

3. 4.

Figures 3, 4. **(3)** Normal, water, and fat sagittal images of the right knee of a healthy volunteer. Two of five simultaneously acquired 5-mm sections are shown. **(4)** Normal, water, and fat sagittal images of the spine of a healthy volunteer. Two of eight simultaneously acquired 5-mm sections are shown.

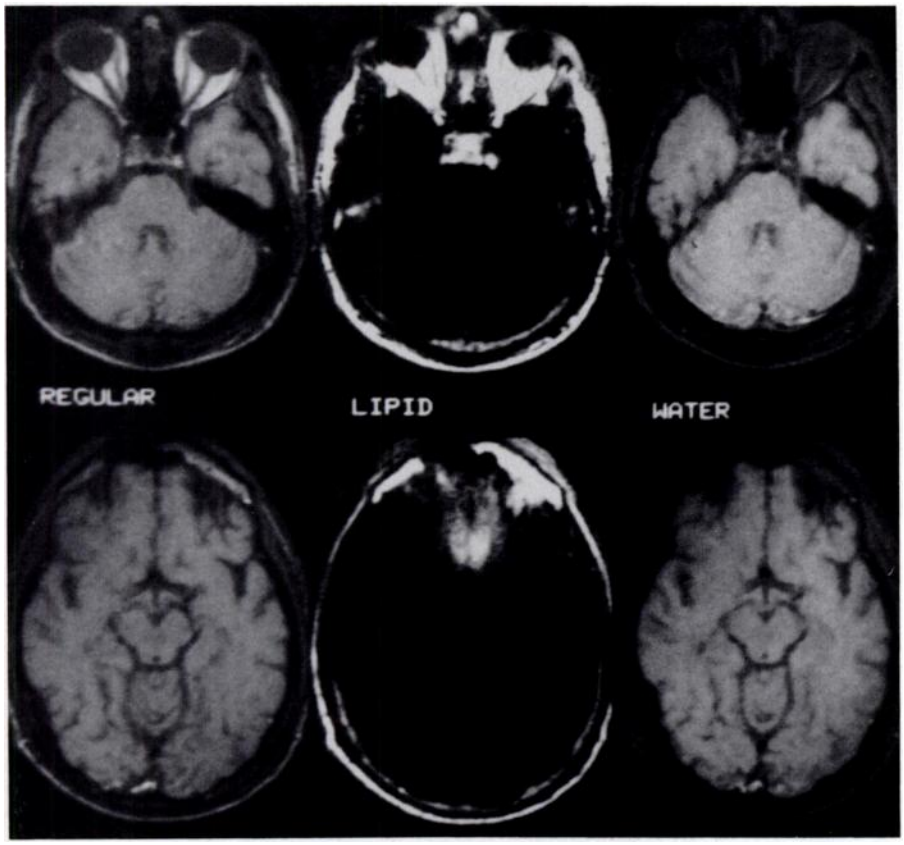

Figure 5. Normal, fat, and water axial images of the head of a healthy volunteer acquired with a volume head coil. Two of five simultaneously acquired 3-mm sections are shown.

image in the region of the ethmoid sinus in Figure 5. B_1 inhomogeneity will cause variation in the degree of suppression of the undesired resonance because of deviation of the flip angle of the presaturation pulse from $\pi/2$. This probably accounts for the apparent decrease in the fat-water separation observed in the images of the spine. It is clear, though, that multisection chemical shift imaging can be implemented on high-field whole-body MR imaging systems with minimal modification of standard imaging technology. ■

References

1. Bottomley PA, Foster TH, Leue WM. In vivo nuclear magnetic resonance chemical shift imaging by selective irradiation. Proc Natl Acad Sci USA 1984; 81:6856–6860.
2. Hall LD, Sulumar S, Talagala SL. Chemical shift resolved tomography using frequency selective excitation and suppression of specific resonances. J Magn Reson 1984; 56:275–278.
3. Haase A, Frahm J. Multiple chemical-shift-selective NMR imaging using stimulated echos. J Magn Reson 1985; 64:94–102.
4. Dumoulin CL. A method for chemical shift selective imaging. Magn Reson Med 1985; 2:583–585.
5. Axel S, Dougherty L. Chemical shift selective magnetic resonance imaging of multiple line spectra by selective saturation. J Magn Reson 1985; 66:194–196.
6. Dixon WT. Simple proton spectroscopic imaging. Radiology 1984; 153:189–194.
7. Axel L, Glover G, Pelc N. Chemical shift magnetic resonance imaging of two-line spectra by gradient reversal. Magn Reson Med 1985; 2:428–436.
8. Twieg DR, McKinnon GC. Multiple output chemical shift imaging (MOCSI): a rapid method for chemical shift imaging and localized moderate resolution NMR spectroscopy. Magn Reson Imaging 1986; 4:118.
9. Dumoulin CL. A multiple quantum filter for the imaging of homonuclear spin-spin coupled nuclei. In: Book of abstracts: Society of Magnetic Resonance in Medicine 1985. Vol. 1. Berkeley, Calif.: Society of Magnetic Resonance in Medicine, 1986; 145–146.
10. Guilfoyle DN, Mansfield P. Chemical shift imaging. Magn Reson Med 1985; 2:479–489.
11. Ahn CB, Lee SY, Nalcioglu O, Cho ZH. Spectroscopic imaging by quadrature modulated echo time shifting. Magn Reson Imaging 1986; 4:110.
12. Yeung HN, Kormos DW. Separation of true fat and water images by correcting magnetic field inhomogeneity in situ. Radiology 1986; 159:783–786.
13. Redfield AG, Gupta RK. Pulsed Fourier transform NMR spectrometer for use with H_2O solutions. J Chem Phys 1971; 54:1418–1419.